THE JOURNAL OF PHYSICAL CHEMISTRY B

Article

pubs.acs.org/JPCB

Molecular Anion Hydrogen Bonding Dynamics in Aqueous Solution

Rongfeng Yuan, Chang Yan, Amr Tamimi, and Michael D. Fayer*

Department of Chemistry, Stanford University, Stanford, California 94305, United States

ABSTRACT: The dynamic nature of hydrogen bonding between a molecular anion, selenocyanate ($SeCN^-$), and water in aqueous solution (D_2O) is addressed using FT-IR spectroscopy, two-dimensional infrared (2D IR) vibrational echo spectroscopy, and polarization selective IR pump−probe (PSPP) experiments performed on the CN stretching mode. The CN absorption spectrum is asymmetric with a wing on the low frequency (red) side of the line in contrast to the spectrum in the absence of hydrogen bonding. It is shown that the red wing is the result of an increase in the CN stretch transition dipole moment due to the effect of hydrogen bonding (non-Condon effect). This non-Condon effect is similar in nature to observations on pure water and other nonionic systems where hydrogen bonding enhances the extinction coefficient. The 2D IR measurements of spectral diffusion (solvent structural evolution) yield a time constant of 1.5 ps, which is within error the same as that of the OH stretch of HOD in D_2O (1.4 ps). The orientational relaxation of $SeCN^-$ measured by PSPP experiments is long (4.04 ps) compared to the spectral diffusion time. The population decay at or near the absorption line center is a single-exponential decay of 37.4 ± 0.3 ps, the vibrational lifetime. However, on the red side of the line the decay is biexponential with a low amplitude, fast component; on the blue side of the line there is a low amplitude, fast growth followed by the lifetime decay. Both of the fast components have 1.5 ps time constants, which is the spectral diffusion time. The fast components of the population decays are the results of the non-Condon effect that causes the red side of the line to be over pumped by the pump pulse. Spectral diffusion then produces the fast decay component on the red side of the line and the growth on the blue side of the line as the excess initial population on the red side produces a net population flow from red to blue.

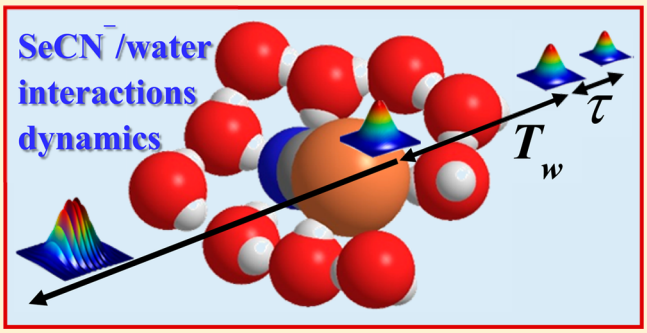

I. INTRODUCTION

Water is a small molecule with unusual properties that arise from its extended hydrogen bond network. For example, water's melting point (273 K) and boiling point (373 K) are significantly higher than those of methane (91 and 112 K), even though the two molecules have similar molecular masses and volumes. The difference is caused by water's hydrogen bonds. Water's hydrogen bond network is not static; it constantly undergoes rapid rearrangement on the time scale of picoseconds.[1−6] The hydroxyl stretch of water can be used as a vibrational probe of water dynamics which occur on ultrafast time scales. Two-dimensional infrared (2D IR) vibrational echo experiments that measure spectral diffusion, which is caused by the structural evolution of a system, reveal that the hydrogen bond dynamics in pure water occur on two time scales of 400 fs and 1.7 ps (340 fs and 1.4 ps for D_2O), which are caused by hydrogen bond length fluctuations and the complete randomization of the hydrogen bond network, respectively.[3,5−8] In addition there are ultrafast motions (~50 fs) that are responsible for the homogeneous component of the absorption spectrum.[6]

Water exists in a vast number of systems other than pure bulk water. Water molecules in aqueous ionic solutions,[8−12] in the nanopools of reverse micelle (RM),[13−15] mixed with other solvents,[16,17] in ionic liquids,[18−20] and in the nanochannels of polyelectrolyte fuel cell membranes[21,22] have altered hydrogen bond networks with distinct dynamics. Aqueous salt solutions have attracted a great deal of interest because they are ubiquitous in our environment, industry, and living cells. A substantial amount of research, both theoretical and experimental, has been focused on the effects of ions on hydrogen bonding dynamics. By employing nuclear magnetic resonance (NMR),[23] ultrafast IR spectroscopy,[8,24−27] and molecular dynamics (MD) simulations,[28−30] researchers have generally observed slower hydrogen bond dynamics for water in the proximity of ions. In the ultrafast IR experiments, the hydrogen bond dynamics were studied using the hydroxyl stretch as a probe. To examine anion−water interactions, neutron scattering was used to characterize the hydration shell structure, and the existence of hydrogen bonds between water and solvated halide ions or thiocyanate anions was confirmed.[31−33]

While dynamics of water interacting with anions has been studied from the perspective of the water molecules, there is little information on the anion−water hydrogen bond interactions from the perspective of the anions, although there is a recent study of borohydride anion in D_2O using the triply degenerate B−H stretch as the vibrational probe.[12] The heavily studied halide ions in aqueous solutions obviously

Received: August 21, 2015
Revised: September 30, 2015
Published: October 4, 2015

DOI: 10.1021/acs.jpcb.5b08168
J. Phys. Chem. B 2015, 119, 13407−13415

cannot be studied using vibrational experiments, although there have been X-ray experiments that examined the structure of water around halides.[26,34,35] However, polyatomic anions can be investigated with the full range of IR experiments. The selenocyanate ion, $SeCN^-$, distinguishes itself from other anions by its IR-active CN group that has a long vibrational lifetime. Indeed, $SeCN^-$ has been used as an IR probe in bulk solution previously, but the aims of these prior studies were to detect contact ion pair dynamics in very concentrated dimethylformamide (DMF) solutions[36] or to determine the vibrational energy transfer rate among anions again with very high $SeCN^-$ concentrations.[37]

The impacts on an anion of hydrogen bonds with water are investigated here by studying dilute aqueous solutions of KSeCN (potassium selenocyanate). The investigations use FT-IR spectroscopy, two-dimensional infrared vibrational echo spectroscopy, and polarization selective IR pump−probe (PSPP) experiments. The linear IR absorption spectrum of the CN stretch shows a mildly asymmetric peak with a wing on the red (low frequency) side of the line that is not present in a system lacking water−$SeCN^-$ hydrogen bonding. In bulk water, the hydroxyl stretch absorption spectrum is asymmetric, again with a wing on the red side of the line. For example, the wing is evident in the OD stretch of HOD in H_2O.[1−6] In water, the asymmetry of the hydroxyl stretch is induced by "non-Condon effect".[38,39] In vibrational spectroscopy, the Condon approximation is frequently applied; that is, the vibrational transition dipole is constant, independent of the translational and rotational coordinates of the molecules in the liquid.[38] However, in bulk water the strong hydrogen bonds have an appreciable effect on both the frequency and the transition dipole of the hydroxyl stretch.[39] Stronger hydrogen bonds shift the absorption frequency to the red and increase the transition dipole. The result is more absorption on the red side of the line than the concentration alone would dictate, resulting in the red wing.

In water, the hydroxyl is the hydrogen bond donor. Selenocyanate is a hydrogen bond acceptor. Can the red wing in the selenocyanate CN vibrational spectrum be caused by the non-Condon effect? This question is answered, and substantial information is obtained about water−anion hydrogen bond dynamics and interactions by applying both 2D IR experiments and IR pump−probe experiments. The 2D IR experiments on the CN stretch give a spectral diffusion time (the time-dependent evolution of frequency of the vibration mode caused by structural evolution of the medium) that is identical to the hydrogen bond network rearrangement spectral diffusion time measured for D_2O, within experimental error (1.5 ± 0.2 ps for CN vs 1.4 ± 0.2 ps for the OH stretch of HOD in D_2O).[7] Polarization selective pump−probe measurements yield a $SeCN^-$ orientational relaxation time of 4.04 ps and a vibrational lifetime of 37.4 ± 0.3 ps. At the center of the absorption spectrum, the population decay is single exponential with this lifetime. However, on the blue and red sides of the line at short time, the decays are not single exponential. On the red side of the line, the decay is biexponential with the long component equal to the lifetime. On the blue side of the line, the data show a growth at short time followed by the lifetime decay. These fast components can be well modeled using the spectral diffusion rate measured by the 2D IR experiments. Because of the non-Condon effect, the red side of the line is overpumped. Excited state population then undergoes spectral diffusion. At short time there is a net flow of population from the red side to the blue side of the line. The population distribution comes to equilibrium with the spectral diffusion time and subsequently decays with the vibrational lifetime.

II. EXPERIMENTAL METHODS

A. Sample Preparation. Experiments were conducted on KSeCN in bulk water and in very small AOT (dioctyl sulfosuccinate sodium salt) reverse micelles. KSeCN, AOT, and isooctane were obtained from Sigma-Aldrich and were used as received without further purification. The bulk water KSeCN samples were 0.5 M solution in D_2O. D_2O was used rather than H_2O because of the overlap of the large O−H stretch band of H_2O and the CN stretch band. For AOT reverse micelle samples, a 1 M isooctane solution of AOT was prepared by weight, and the water content was determined by Karl Fischer titration. The proper amount of D_2O was added to the AOT solution to prepare w_0 = 1 reverse micelle (one water molecule per surfactant molecule). Samples were assembled by placing a portion of the solution between two CaF_2 windows separated by a Teflon spacer of sufficient thickness so that the absorbance was between 0.1 and 0.2.

Infrared spectra were taken with a Thermo Scientific Nicolet 6700 FT-IR spectrometer. The spectra of identical samples, but made without adding KSeCN, were subtracted from the sample spectra to give the spectra of the CN stretch alone.

B. 2D IR and Polarization Selective Pump−Probe Experiments. Both 2D IR and PSPP measurements were performed with pump−probe geometry using the same optical platform. Details of the setup have been reported previously;[40] here a brief description is presented. A home-built mid-IR optical parametric amplifier, which was pumped by a Ti:sapphire regenerative amplifier, produced ∼170 fs pulses centered at 2075 cm^{-1} with ∼8 μJ pulse energy. The mid-IR pulses were split into a weaker probe pulse and a stronger pump pulse. The weak pulse was routed through a mechanical delay line which was used to set the waiting time T_w for the 2D IR experiments (see below) and the delay time in the PSPP experiments. The strong pulse was sent to an acousto-optic mid-IR Fourier-domain pulse shaper.[40] The output beam from the pulse shaper, which generated pulses 1 and 2 in the 2D IR experiments and the single pump pulse in the PSPP experiments, was crossed in the sample with the probe pulse. The probe pulse, which carried the signal in pump−probe and vibrational echo experiments, was sent to a spectrometer equipped with a 32-element HgCdTe (MCT) IR array detector. In the 2D IR experiments, the pulse shaper was used to make two of the three excitation pulses (1 and 2) and control their delay and phase (phase cycling). In the PSPP experiments the pulse shaper was used to chop the pump pulse and for phase cycling. In both experiments, the phase cycling removes scattered light from the pump that can interfere with measurements of small signals on the probe.

In a 2D IR experiment, three excitation pulses impinge on the sample with controllable time delays. The nonlinear interaction of the three pulses with the vibrational probe molecules ($SeCN^-$) generates a fourth pulse, the vibrational echo. The time between pulses 1 and 2 is τ, and the time between pulses 2 and 3 is T_w. The vibrational echo pulse is emitted at a time $\leq \tau$ after pulse 3.

The two pump pulses (1 and 2) label all of the vibrational oscillators with their initial frequencies. During the time period T_w, the structure of the system evolves. Then pulse 3 generates the vibrational echo signal that reads out the frequencies of the

DOI: 10.1021/acs.jpcb.5b08168
J. Phys. Chem. B 2015, 119, 13407−13415

vibrational oscillators after the system has had the period T_w to evolve. The vibrational echo signal propagates collinearly with the pulse 3, which serves as the local oscillator (LO) to detect the phase of the echo signal.

The 2D IR spectra require two Fourier transforms to go from the time domain to the frequency domain. The spectrograph performs one of the Fourier transforms experimentally by resolving the echo/LO pulse into its composite frequencies giving the ω_m (vertical axis) of the 2D spectrum. The horizontal axis, ω_τ, is obtained by scanning τ; when τ is scanned, the echo moves in time relative to the fixed LO, producing an interferogram. The interferogram, recorded at each ω_m, is numerically Fourier transformed to give the ω_τ axis of the 2D spectrum

For each T_w, τ is scanned and a 2D IR spectrum is obtained. The spectral diffusion (and thus the structural evolution) is extracted from the evolution of the 2D band shape at each T_w. At short T_w, the detection frequency (ω_m) is approximately the same as the excitation frequency (ω_τ), giving a spectrum that is elongated along the diagonal (upper right to lower left corners of the 2D spectrum). The shape of the spectrum becomes more symmetrical as spectral diffusion (structural evolution) progresses, which causes the initial and final frequencies to be less correlated; the spectrum will be completely round when all structures have been sampled during the period T_w.

The results of the 2D IR experiments are analyzed in terms of the frequency−frequency correlation function (FFCF), which quantifies the spectral diffusion in terms of the frequency fluctuation amplitudes and time constants. The FFCF is the probability that a vibration with an initial frequency in the inhomogeneous spectral distribution still has the same frequency at a later time, averaged over all initial frequencies. To extract the FFCF from the 2D spectra, the center line slope (CLS) analysis was employed.[41,42] A fit to the CLS vs T_w curve, which is the normalized FFCF, gives spectral diffusion time constants and amplitude factors. The FFCF is described with a multiexponential model:

$$C_1(t) = \langle \delta\omega(t)\delta\omega(0)\rangle = \sum_i \Delta_i^2 \exp(-t/\tau_i) \tag{1}$$

Here, $\delta\omega(t) = \omega(t) - \langle\omega\rangle$ is the instantaneous frequency fluctuation with $\langle\omega\rangle$ the average frequency. Δ_i is the frequency fluctuation amplitude of each component, and τ_i is its associated time constant. A component of the FFCF with $\Delta_i\tau_i < 1$ is motionally narrowed. When a component is motionally narrowed, Δ and τ cannot be determined separately. The motionally narrowed homogeneous contribution to the absorption spectrum has a pure dephasing line width given by $\Gamma^* = \Delta^2\tau = 1/\pi T_2^*$, where T_2^* is the pure dephasing time. The observed homogeneous dephasing time, T_2, also has contributions from the vibrational lifetime and orientational relaxation:

$$\frac{1}{T_2} = \frac{1}{T_2^*} + \frac{1}{2T_1} + \frac{1}{3T_{or}} \tag{2}$$

where T_2^*, T_1, and T_{or} are the pure dephasing time, vibrational lifetime, and orientational relaxation times, respectively. The total homogeneous line width is $\Gamma = 1/\pi T_2$. In our case, the total homogeneous line width is 26.6 cm^{-1}, while the contributions from vibrational lifetime and orientational relaxation are 0.1 and 0.9 cm^{-1}, respectively (see Results and Discussion). Therefore, pure dephasing is the dominant contribution. The total homogeneous dephasing time T_2 and the values of Δ_i in units of frequency are obtained from the experimental data by a simultaneous fit to the CLS decay and the experimental linear absorption line shape.[40]

The polarization selective pump−probe experiments track the decay of the probe transmission with polarizations parallel and perpendicular to the pump pulse polarization. The parallel and perpendicular components of the probe signal, $S_\parallel(t)$ and $S_\perp(t)$, can be expressed in terms of population relaxation, $P(t)$, and the orientational relaxation correlation function, $C_2(t)$, which is the second Legendre polynomial correlation function.

$$S_\parallel(t) = P(t)[1 + 0.8C_2(t)] \tag{3}$$

$$S_\perp(t) = P(t)[1 - 0.4C_2(t)] \tag{4}$$

Then, the population relaxation and orientational relaxation are

$$P(t) = S_\parallel(t) + 2S_\perp(t) \tag{5}$$

$$r(t) = \frac{S_\parallel(t) - S_\perp(t)}{S_\parallel(t) + 2S_\perp(t)} \tag{6}$$

$r(t)$ is the anisotropy. $r(t) = 0.4C_2(t)$. In the experiment, the polarization of the probe was horizontal. A half wave plate and a polarizer set the polarization of pump to 45° relative to the probe. Following the sample, the probe pulse was resolved either parallel or perpendicular to the polarization of the pump using a polarizer in a computer-controlled rotation mount. Care was taken to make sure the probe spectra in the parallel and perpendicular polarizations were identical in amplitude in the absence of the pump pulse.

III. RESULTS AND DISCUSSION

A. Absorption Spectra. In Figure 1, FT-IR spectra of the CN stretch of $SeCN^-$ in 0.5 M bulk D_2O solution (A) and in $w_0 = 1$ AOT reverse micelles (B) are shown. In contrast to the bulk water solution, in the $w_0 = 1$ reverse micelles there is so little water that a negligible number of selenocyanates will have even one water molecule hydrogen bonded to it. There are not enough water molecules to hydrate the AOT sulfonate head groups, which require ∼4−6 water molecules per head group for complete hydration.[43] In addition, according to MD simulations performed by Ladanyi and co-workers, in the smallest $w_0 = 1$ reverse micelle, the interfacial region is a structured arrangement of Na^+, H_2O, and sulfonate head groups that only breaks up with increased hydration.[44] Therefore, we use the spectrum in the $w_0 = 1$ RM as the spectrum in the absence of water hydrogen bonding to the $SeCN^-$.

In Figure 1A, the dashed red curve is a fit to a Voigt line shape function on the blue side of the spectrum to the peak of the spectrum. The fit curve is then extended to the red side of the spectrum. This fit shows that the spectrum of selenocyanate in water is not symmetrical. It has a small wing on the red side of the line. The red dashed curve in Figure 1B is a Voigt fit to the spectrum in the $w_0 = 1$ AOT reverse micelles. The fit is essentially perfect, showing that the absorption line is symmetric in the absence of hydrogen bonding to water. As a further check, the spectrum (not shown) of selenocyanate in a very dry (∼1 ppm water) room temperature ionic liquid also has a symmetric Voigt line shape.

Therefore, it is reasonable to assume that the asymmetric shape of the absorption spectrum in water is caused by the

DOI: 10.1021/acs.jpcb.5b08168
J. Phys. Chem. B 2015, 119, 13407−13415

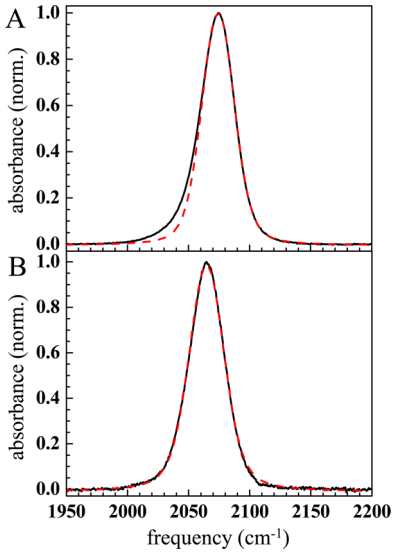

Figure 1. FT-IR spectra of the CN stretch of $SeCN^-$ in two different systems. (A) Normalized IR absorption spectrum in bulk D_2O solution. The black solid curve is the measured data while the red dashed curve is a fit to a Voigt function on the high frequency (blue) side of the line to the peak of the spectrum. The fit curve is extended on the red side of the line, revealing the "wing" on the red side of the line. (B) Normalized IR absorption spectrum in w_0 = 1 AOT reverse micelles. The black solid curve is the measured data, and the red dashed line is the fit to a Voigt function. In the absence of hydrogen bonding to the $SeCN^-$, the spectrum is symmetrical.

hydrogen bonding of water to the anions. As discussed in the Introduction, the asymmetric line shape of the hydroxyl stretch of water in bulk water is caused by the non-Condon effect.[5,45] In water, stronger hydrogen bonds enhance absorption on the red side of the line relative to the blue side of the line. However, for the CN stretch, it is known that hydrogen bonding shifts the vibrational frequency to the blue.[46] This result suggests that for $SeCN^-$ weaker hydrogen bonds will be associated with the red side of the line. Then, the non-Condon red wing of the absorption spectrum of $SeCN^-$ in water is likely attributable to weaker hydrogen bonds with water molecules. This is the opposite of the situation for hydroxyls in water.

A qualitative explanation involves the nature of the bonding in $SeCN^-$. $SeCN^-$ bonds have contributions from two resonance structures: $[Se{-}C{\equiv}N]^-$ and $[Se{=}C{=}N]^-$. When hydrogen bonds formed between the lone pair of nitrogen atom in $SeCN^-$ and water, the electron density in $SeCN^-$ shifts toward the nitrogen atom. The hydrogen bonds will cause the $SeCN^-$ structure to have a greater contribution from the $[Se{-}C{\equiv}N]^-$ resonance structure, and stronger hydrogen bonds will increase the contribution from the triple bond resonance structure. $[Se{=}C{=}N]^-$ absorbs at lower frequency and, for $SeCN^-$ hydrogen bonded to water, has a stronger transition dipole than $[Se{-}C{\equiv}N]^-$. Therefore, weaker hydrogen bonds produces more double bond character, a red-shift, and a stronger transition dipole, giving rise to the non-Condon red wing.

This proposal is supported by examining the vibrational spectra of CN^- and SCN^-. In the case of cyanide anion, in which a pure triple bond exists between C and N, the absorption peak is at 2080 cm^{-1} in D_2O, which is to the blue of the CN stretch of $SeCN^-$. The transition dipole of $SeCN^-$ was measured to be 3.4 times stronger than that of CN^-. For thiocyanate anion, which is known to be dominated by $[S{=}C{=}N]^-$,[31] the peak is at 2065 cm^{-1} in D_2O, to the red of the CN stretch of $SeCN^-$, and the transition dipole was measured to be 1.4 times stronger than that of $SeCN^-$. The interactions between $SeCN^-$ and water molecules can span a wide range of configurations with different hydrogen bonding strengths, as evidenced by the inhomogeneously broadened absorption line. Various hydrogen bond strengths can lead to the variation of the transition dipole across the absorption line.

The hydrogen bonding of water to $SeCN^-$ plays a role in the variation in the transition dipole across the absorption line and in enhancing the transition dipole. $SeCN^-$ in aqueous solution has higher absorption frequency (2075 cm^{-1}) than that in the w_0 = 1 AOT reverse micelle (2065 cm^{-1}) where hydrogen bonding with water is absent. The red-shift of the absorption in the reverse micelles suggests more double bond character. However, the transition dipole of $SeCN^-$ in water is ~1.25 time greater than it is in the reverse micelles. Two possibilities may explain the decrease in the transition dipole in the reverse micelles. The transition dipole depends on the dipole moment derivative, that is, the change in dipole with bond length. When the bonding is a mix of double and triple bond character, a change in bond length can change the double/triple mix to produce a change in the dipole that is larger than that which occurs for a pure triple or pure double bond. It is possible that in the reverse micelle the bonding is so dominated by the double bond resonance structure that the change in bond length does not result in a significant change in the mix of resonance structures. $SeCN^-$ and SCN^- may be in a sweet spot where the mix of resonance structures and the associated change in dipole is particularly sensitive to the bond length. The other possibility is the participation of the hydrogen bonded water in the dipole derivative. When the bond length changes, the hydrogen bonding interactions will change, which can contribute to a change in dipole that is not possible in the absence of hydrogen bonding in the w_0 = 1 reverse micelles.

In water, the hydroxyl is a hydrogen bond donor. Here, the $SeCN^-$ is a hydrogen bond acceptor. The dynamical experiments presented below confirm that the asymmetry observed for the selenocyanate spectrum in water is caused by the non-Condon effect. The results show that an anion acceptor of water hydrogen bonds can also have its transition dipole altered through hydrogen bonding to water.

B. Time-Dependent Experiments. Figure 2 shows the results of the 2D IR experiments on the CN stretch of $SeCN^-$ in D_2O. The inset has two of the 2D IR spectra at T_w = 0.5 ps and T_w = 10.0 ps. One can clearly see that 2D spectrum changes shape when the time increases, becoming less elongated along the diagonal (dashed black line in the upper panel) at the longer T_w. The main part of the figure shows CLS data (black circles). Each point in the plot is the CLS of a 2D IR spectrum at one T_w. The CLS decay is the normalized FFCF. The difference between the value of the CLS curve and 1 at T_w = 0 is a measure of the homogeneous line width. As discussed in section II, using the CLS and the linear absorption spectrum, the full FFCF, including the homogeneous component and the amplitudes (Δ_i) in frequency units in eq 1, is obtained. The solid red curve is a single-exponential fit to the data. The decay time, which is the time constant for spectral diffusion, is 1.5 ± 0.2 ps. Using the CLS analysis, the homogeneous and inhomogeneous line widths are 26.6 and 15.5 cm^{-1}, respectively. The convolution of these components

DOI: 10.1021/acs.jpcb.5b08168
J. Phys. Chem. B 2015, 119, 13407−13415

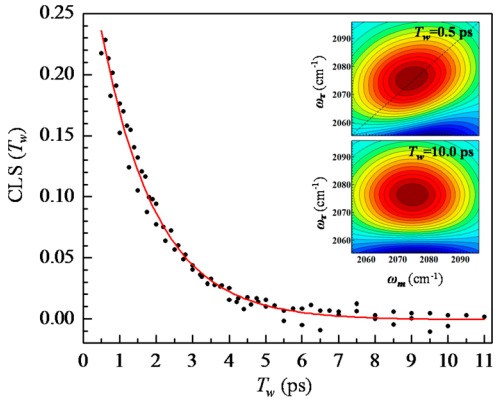

Figure 2. CLS (the normalized FFCF) decay (black circles) extracted from the 2D IR spectra of the CN stretch of $SeCN^-$ in D_2O solution. The solid red curve is a single-exponential fit to the data that yields a spectral diffusion time constant of 1.5 ps. The inset shows 2D IR spectrum at T_w = 0.5 ps and T_w = 10.0 ps.

gives the total absorption full width at half-maximum (fwhm) line width of 33.0 cm^{-1}.

Figure 3 displays the PSPP anisotropy decay data, $r(t)$, obtained using eq 6. The red curve is a single-exponential fit to

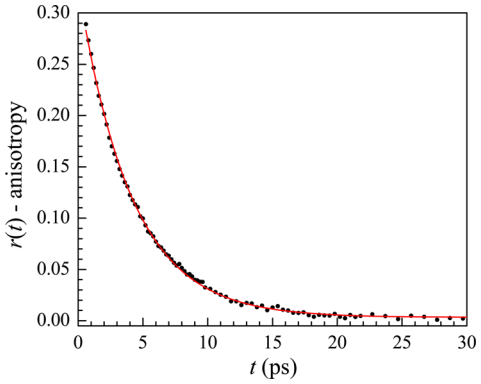

Figure 3. Anisotropy (orientational relaxation) decay (black circles) of $SeCN^-$ in D_2O solution obtained from polarization selective pump–probe measurements. The solid red curve is a single-exponential fit to the data that yields an anisotropy decay time constant of 4.04 ps.

the data, which yields an orientational relaxation time of 4.04 ± 0.04 ps. The orientational relaxation is slow compared to the spectral diffusion. Therefore, orientation relaxation of the $SeCN^-$ is not the source of the 1.5 ps spectral diffusion. The difference between the value of $r(t)$ and 0.4 at t = 0 is caused by ultrafast inertial orientational motions, which are not resolvable.

Figure 4A is the population relaxation, $P(t)$, from eq 5 taken at the line center. The solid red curve is a single-exponential fit to the data, which yields a vibrational lifetime of 37.4 ± 0.3 ps (see more below). From eq 2, the orientational relaxation contributes 0.9 cm^{-1} and the vibrational lifetime contributes 0.1 cm^{-1} to the homogeneous line width of 26.6 cm^{-1}. Therefore, the homogeneous line width is dominated by pure dephasing, that is, ultrafast structural fluctuations that are motionally narrowed.

The 1.5 ps spectral diffusion time constant measured, with the CN stretch of $SeCN^-$ as the vibrational probe, is the same, within experimental error, as the slowest component of hydrogen bond dynamics of the OH stretch of HOD in D_2O, which is 1.4 ± 0.2 ps.[7] A small amount of HOD in D_2O

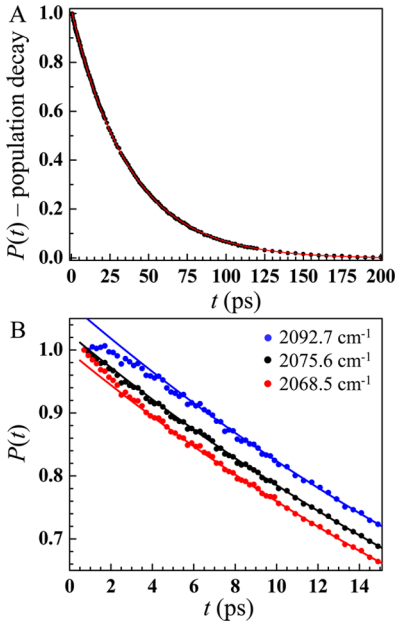

Figure 4. (A) Population decay of the CN stretch of $SeCN^-$ (black circles) taken at a frequency near the center of the absorption line. The red curve is a single-exponential fit to the data and yields a vibrational lifetime of 37.4 ± 0.3 ps. (B) The short time pump–probe decays at three wavelengths (circles). The solid curves are single 37.4 ps exponentials. On the red side of the line (red circles) there is a fast decay component. On the blue side of the line (blue circles) there is an increase in signal at short time.

does not change the D_2O dynamics.[47] Since the spectral diffusion is determined by all of the dynamic hydrogen bond interactions with the D_2O molecules that surround the HOD, this measurement is a determination of the D_2O dynamics.[47] The slowest component of the spectral diffusion has been shown via MD simulations to be associated with the complete randomization of the hydrogen bond network.[5,6] Given that the $SeCN^-$ spectral diffusion is essentially identical to the OH stretch of HOD in D_2O spectral diffusion, and the reorientation of $SeCN^-$ itself is negligible on this spectral diffusion time scale, it is reasonable to conclude that the spectral diffusion sensed by the anion is caused by the randomization of the D_2O hydrogen bonding network.

Hydroxyls in water are hydrogen bond donors. In contrast, $SeCN^-$ is a hydrogen bond acceptor. The selenocyanate hydrogen bond acceptor senses the frequency fluctuations caused by the hydrogen bond network randomization as does the hydroxyl of HOD. However, there are major differences in how OH and $SeCN^-$ experience their D_2O environments. The CN stretch of $SeCN^-$ absorption spectrum in D_2O has a fwhm of 33 cm^{-1} while the OH stretch of HOD in D_2O has a fwhm of 260 cm^{-1}.[7] Thus, the hydroxyl stretch frequency is much more sensitive to differences in the hydrogen bond network structure than the CN stretch of selenocyanate. The 2D IR experiments on OH of HOD in D_2O and OD of HOD in H_2O both show large amplitude fast spectral diffusion of ~400 fs.[5−7] The experiments on HOD in D_2O and H_2O used very short IR pulses of ~50 fs. Here the pulse duration was 170 fs, but it should still have been possible to observe an ~400 fs large amplitude component. In the experiments on the hydroxyl stretch, the MD simulations show that the fast component is caused by very local hydrogen bond fluctuations, mainly hydrogen bond length fluctuations.[6] The hydroxyl donor

DOI: 10.1021/acs.jpcb.5b08168
J. Phys. Chem. B 2015, 119, 13407−13415

frequency is very sensitive to the strength of the hydrogen bond which is directly correlated with the length of the hydrogen bond. The apparent absence of a very fast component in the selenocyanate spectral diffusion may indicate that $SeCN^-$ hydrogen bond acceptor is not sensitive to the hydrogen bond lengths but is sensitive to the global rearrangement of the entire hydrogen bonding network.

It is also possible that the hydrogen bond length fluctuations of water bound to $SeCN^-$ are much faster than 400 fs and too fast to resolve with the pulse duration used here. Another possibility is that the fluctuations are fast relative to the range of frequencies associated with them. If this is the case, the sampling of these frequencies will be motionally narrowed ($\Delta\tau < 1$), and the frequency fluctuations are part of the homogeneous line width. The width, Δ in eq 1, of the fast spectral diffusion component of the hydroxyl stretch in water is ~60 cm^{-1}. For heuristic purposes, if we scale this value down by the ratio of the absorption line widths, 33/260, and use the time constant for the fast spectral diffusion component of OH in D_2O of 340 fs, $\Delta\tau$ = ~0.5. Thus, the fast component of the fluctuations for selenocyanate would be part of the homogeneous line width and not show up as a component of the spectral diffusion.

Returning to the pump−probe data, it provides direct evidence for the non-Condon effect that was proposed to explain the asymmetric absorption line shape shown in Figure 1A. As discussed above, Figure 4A shows $P(t)$ and a single-exponential fit to the data taken at approximately the line center, 2075.6 cm^{-1}. As can be seen in Figure 4A, the decay is a single exponential. Figure 4B shows the short time $P(t)$ data at three wavelengths. The black points are the same data as in Figure 4A. The lines through the data are single-exponential fits that start after 10 ps. All of these fits give the same decay time within experimental error, 37.4 ps. However, it is clear that the data on the blue side of the line (blue points) and on the red side of the line (red points) are not single exponentials at short time, <~6 ps. On the red side of the absorption spectrum, there is an initial fast decay, and on the blue side of the spectrum there is an increase in the signal before it goes into the lifetime decay.

Figure 5 shows the same data as in Figure 4B but with fits that include the short time portions. The black points, taken near line center, are fit well at all times with a single-exponential decay. The data on the red side of the line (red circles) and the data on the blue side of the line (blue circles) are fit with the following two equations, respectively.

$$P_r(t) = A_1 \exp(-t/\tau_1) + A_2 \exp(-t/\tau_2) \quad (7)$$

$$P_b(t) = A_1(1 - \exp(-t/\tau_1)) \exp(-t/\tau_2) + A_2 \exp(-t/\tau_2) \quad (8)$$

where the subscripts r and b stand for red and blue. The fitting procedure fixed the two time constants at the spectral diffusion value, 1.5 ps, and the lifetime, 37.4 ps, with only the amplitude factors, A_1 and A_2, allowed to float. As can be seen in Figure 5, this procedure reproduces the curves extremely well. If the fast component τ_1 is also allowed to float, the results yield the spectral diffusion time within the experimental error.

The IR frequency was tuned to the peak of the CN stretch absorption spectrum, and the pulse bandwidth, 110 cm^{-1}, is large enough to be considered uniform across the CN stretch spectrum, which has a line width of 33 cm^{-1}. The non-Condon effect can explain the data and the fitting results. Prior to vibrational excitation by the pump pulse, the system is in the ground state and in thermal equilibrium. There are a wide variety of liquid configurations that give rise to different transition energies. These configurations have equilibrium populations that are determined by their probability of occurrence. Any selenocyanate will see its surrounding D_2O configuration change with time, but the probabilities of finding the various configurations for the ensemble is time independent. The number of ground state molecules moving from blue to red transition frequencies is the same as the number moving from red to blue.

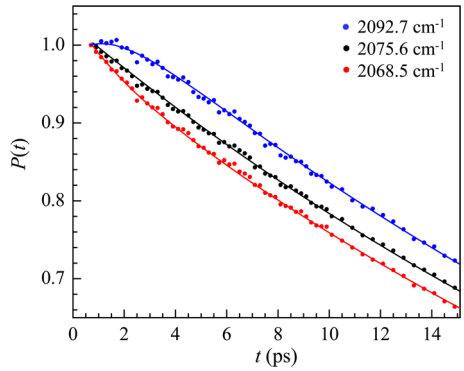

Figure 5. Same data as in Figure 4B (circles) and fits to the data. At the center frequency (black circles and black solid curve fit), the data are a single-exponential decay with the lifetime. On the red side of the spectrum, the fit (red curve) is a biexponential. On the blue side, the fit is a growth and decay (see eqs 7 and 8). In both of these, the time constants are fixed at the spectral diffusion time (1.5 ps) and the lifetime (37.4 ps). Only the relative amplitudes of the two components were allowed to float in the fits.

In the discussion of the wing on the red side of the absorption line seen in Figure 1A, it was proposed that the wing is caused by molecules with lower transition frequencies having larger transition dipoles than molecules with higher transition frequencies. Because molecules on the red side of the line have larger transition dipoles than those on the blue side, they are "over pumped" by the pump pulse; the number of molecules excited on the red side of the line is greater than it would be based solely on the probability of having structural configurations that give rise to these transition frequencies. Thus, the pump pulses produces a nonequilibrium situation in which, relative to the blue side of the line, there is excess excited state population on the red side of the line. Then initially spectral diffusion will cause more molecules to flow from red to blue than from blue to red. This is necessary to reestablish equilibrium. This flow from red to blue will occur with the spectral diffusion time constant of 1.5 ps. The data in Figure 5 (red circles) have an initial fast decay with the spectral diffusion time constant as the excess excited state population moves from red to blue. The population moving from red to blue initially causes the blue population to increase with the spectral diffusion time constant (blue circles in Figure 5). Near the middle of the line, the red drop and the blue rise cancel, and the decay is a single exponential. The system will establish the equilibrium excited state population distribution after a temporal interval that is several times longer than the spectral diffusion time constant; so for times greater than ~6 ps, the decay at any wavelength is single exponential with the 37.4 ps vibrational lifetime.

DOI: 10.1021/acs.jpcb.5b08168
J. Phys. Chem. B 2015, 119, 13407−13415

The phenomenon of spectral diffusion producing fast decays and buildups in pump−probe experiments with the spectral diffusion times has been observed previously for water and alcohols in room temperature ionic liquids in which the hydroxyl stretch (OD) was excited and probed.[20] It is well-known for hydroxyls that the strength of the hydrogen bond made by the hydroxyl hydrogen bond donor has a strong influence on the transition frequency.[48] Stronger hydrogen bonding in water produces a red-shift and an increase in the transition dipole.[38,39] The spectrum in Figure 1A and the data and fits in Figure 5 provide strong support for the proposition that the hydrogen bond acceptor, $SeCN^-$, also exhibits the non-Condon effect induced by hydrogen bonding, but in a modified manner compared to water. The hydrogen bonds to selenocyanate have a substantially weaker influence on the CN stretch frequency than the hydrogen bonds in bulk water have on the hydroxyl frequency.[31,33,47] The results demonstrate that inhomogeneous broadening of the CN stretch is caused, at least in part, by the strength of hydrogen bonding and that the transition dipole depends on the strength of hydrogen bonding. Weaker hydrogen bonds to $SeCN^-$ shift the frequency to the red and increase the transition dipole, producing the red wing on the absorption line.

IV. CONCLUDING REMARKS

We have examined the nature of the dynamical interactions between a small polyatomic anion and D_2O using time-independent and time-dependent IR spectroscopy of the CN stretch of $SeCN^-$. $SeCN^-$ is a hydrogen bond acceptor for the D_2O hydroxyls. In many respects, the $SeCN^-$ anion has dynamical interactions that are similar to those of a hydroxyl (OH of HOD) in D_2O. Both have asymmetric absorption spectra with a wing on the red side of the absorption line. The combination of absorption experiments and pump−probe experiments show that the red wing on the CN absorption of $SeCN^-$ is caused by the non-Condon effect as is the case for hydroxyls in water (D_2O or H_2O). The $SeCN^-$ anions with weaker hydrogen bonds have lower absorption frequencies and stronger transition dipoles. The transition dipole of the CN stretch increases in magnitude going from the blue side of the line to the red side of the line. These results indicate that the anion, which is a hydrogen bond acceptor, has its absorption frequency and transition dipole influenced by the strengths of the hydrogen bonds to D_2O. The hydroxyl of water is a hydrogen bond donor that is strongly affected by the hydrogen bond strength. The absorption line width of OH of HOD in D_2O is 260 cm^{-1}. The line width of the CN stretch of $SeCN^-$ in D_2O is 33 cm^{-1}. The variation of hydrogen bond strengths to the anion acceptor has much less influence on the vibrational frequency than it does on the hydroxyl hydrogen bond donor. Nonetheless, both the vibrational frequency and transition dipole of the anion acceptor are influenced.

An important result is that the spectral diffusion time reported by the CN stretch of $SeCN^-$ in D_2O is the same as that reported by the OH stretch of low concentration HOD in D_2O. The measurements on the OH stretch in D_2O report on the structural dynamics of the D_2O hydrogen bond network because the low concentration HOD will not change D_2O or H_2O dynamics and MD simulations yield the same dynamics for water with or without HOD.[6,47] The spectral diffusion time measured here, 1.5 ps, corresponds to the randomization of the D_2O hydrogen bond network based on the water simulations. Therefore, the hydrogen bond network dynamics of D_2O surrounding the $SeCN^-$ anion are apparently the same as those of pure D_2O within experimental error. The results imply that the presence of this small polyatomic anion does not substantially change the dynamics of the hydrogen bond network in the vicinity of the anion.

In studies of the influence of ions on water dynamics in which HOD is used as the vibrational probe, high concentrations of ions (salts) are used otherwise the signal is overwhelmed by the bulk water signal.[8,9,11,49] In these types of experiments, the signals are generally a mix of signals from bulk water (if any exists) and water influenced by ions. A typical concentration for which water dynamics significantly deviate from that of bulk water is 6 M. As the concentration is decreased, the measured dynamics approach those of bulk water. For example, in a 2D IR study of NaBr in H_2O solutions using the OD stretch of HOD as a probe and 6, 3, and 1.5 M NaBr concentrations, the slowest spectral diffusion time constants are 4.6, 3.5, and 2.6 ps, respectively. The pure bulk water time constant is 1.7 ps.[8] The approach to the bulk water value at lower concentration is almost certainly due to a larger fraction of the signal coming from water molecules that are not in the vicinity of an anion and are essentially bulk water. Six water molecules are required to solvate a bromide anion. So in 6 M NaBr solution, the vast majority of the water molecules are in the first solvation shell of an anion. These experiments provide information on how water behaves in concentrated solutions in which there is little or no bulk-like water.

The 0.5 M solution of $SeCN^-$ has about 110 water molecules per anion. (Experiments conducted with 0.25 M $SeCN^-$ give the same results.) Thus, there is plenty of water to solvate the anion and to provide a substantial amount of water outside of the solvation shell. Since the signal comes from the $SeCN^-$, the measured dynamics are caused by the solvating water molecules, which are themselves part of the bulk-like water hydrogen bonding network. The results show that at least for this anion its presence does not significantly change the hydrogen bond network randomization dynamics of water.

AUTHOR INFORMATION

Corresponding Author

*E-mail fayer@stanford.edu (M.D.F.).

Notes

The authors declare no competing financial interest.

ACKNOWLEDGMENTS

This work was funded by the Division of Chemical Sciences, Geosciences, and Biosciences, Office of Basic Energy Sciences of the U.S. Department of Energy through Grant DE-FG03-84ER13251 (A.T. and M.D.F.) and the Air Force Office of Scientific Research Grant FA9550-12-1-0050 (R.Y., C.Y., and M.D.F.). C.Y. acknowledges support from Stanford Graduate Fellowships.

REFERENCES

(1) Schuster, P.; Zundel, G.; Sandorfy, C. *The Hydrogen Bond. Recent Developments in Theory and Experiments*; North Holland: Amsterdam, 1976.

(2) Rey, R.; Møller, K. B.; Hynes, J. T. Hydrogen Bond Dynamics in Water and Ultrafast Infrared Spectroscopy. *J. Phys. Chem. A* **2002**, *106*, 11993−11996.

(3) Fecko, C. J.; Eaves, J. D.; Loparo, J. J.; Tokmakoff, A.; Geissler, P. L. Ultrafast Hydrogen-Bond Dynamics in the Infrared Spectroscopy of Water. *Science* **2003**, *301*, 1698−1702.

DOI: 10.1021/acs.jpcb.5b08168
J. Phys. Chem. B 2015, 119, 13407−13415

(4) Rezus, Y. L. A.; Bakker, H. J. On the Orientational Relaxation of HDO in Liquid Water. *J. Chem. Phys.* **2005**, *123*, 114502.
(5) Asbury, J. B.; Steinel, T.; Kwak, K.; Corcelli, S. A.; Lawrence, C. P.; Skinner, J. L.; Fayer, M. D. Dynamics of Water Probed with Vibrational Echo Correlation Spectroscopy. *J. Chem. Phys.* **2004**, *121*, 12431.
(6) Asbury, J. B.; Steinel, T.; Stromberg, C.; Corcelli, S. A.; Lawrence, C. P.; Skinner, J. L.; Fayer, M. D. Water Dynamics: Vibrational Echo Correlation Spectroscopy and Comparison to Molecular Dynamics Simulations. *J. Phys. Chem. A* **2004**, *108*, 1107−1119.
(7) Fecko, C. J.; Loparo, J. J.; Roberts, S. T.; Tokmakoff, A. Local Hydrogen Bonding Dynamics and Collective Reorganization in Water: Ultrafast Infrared Spectroscopy of HOD/D_2O. *J. Chem. Phys.* **2005**, *122*, 054506.
(8) Park, S.; Fayer, M. D. Hydrogen Bond Dynamics in Aqueous NaBr Solutions. *Proc. Natl. Acad. Sci. U. S. A.* **2007**, *104*, 16731−16738.
(9) Bakker, H. J.; Kropman, M. F.; Omata, Y.; Woutersen, S. Hydrogen-Bond Dynamics of Water in Ionic Solutions. *Phys. Scr.* **2004**, *69*, C14−C24.
(10) Omta, A. W.; Kropman, M. F.; Woutersen, S.; Bakker, H. J. Influence of Ions on the Hydrogen-Bond Structure in Liquid Water. *J. Chem. Phys.* **2003**, *119*, 12457−12461.
(11) Giammanco, C. H.; Wong, D. B.; Fayer, M. D. Water Dynamics in Divalent and Monovalent Concentrated Salt Solutions. *J. Phys. Chem. B* **2012**, *116*, 13781−13792.
(12) Giammanco, C. H.; Kramer, P. L.; Fayer, M. D. Dynamics of Dihydrogen Bonding in Aqueous Solutions of Sodium Borohydride. *J. Phys. Chem. B* **2015**, *119*, 3546−3559.
(13) Cringus, D.; Bakulin, A.; Lindner, J.; Vohringer, P.; Pshenichnikov, M. S.; Wiersma, D. A. Ultrafast Energy Transfer in Water-AOT Reverse Micelles. *J. Phys. Chem. B* **2007**, *111*, 14193−14207.
(14) Moilanen, D. E.; Fenn, E. E.; Wong, D.; Fayer, M. D. Water Dynamics in Large and Small Reverse Micelles: From Two Ensembles to Collective Behavior. *J. Chem. Phys.* **2009**, *131*, 014704.
(15) Fenn, E. E.; Wong, D. B.; Fayer, M. D. Water Dynamics in Small Reverse Micelles in Two Solvents: Two-Dimensional Infrared Vibrational Echoes with Two-Dimensional Background Subtraction. *J. Chem. Phys.* **2011**, *134*, 054512.
(16) Harpham, M. R.; Levinger, N. E.; Ladanyi, B. M. An Investigation of Water Dynamics in Binary Mixtures of Water and Dimethyl Sulfoxide. *J. Phys. Chem. B* **2008**, *112*, 283−293.
(17) Wong, D. B.; Sokolowsky, K. P.; El-Barghouthi, M. I.; Fenn, E. E.; Giammanco, C. H.; Sturlaugson, A. L.; Fayer, M. D. Water Dynamics in Water/DMSO Binary Mixtures. *J. Phys. Chem. B* **2012**, *116*, 5479−5490.
(18) Cammarata, L.; Kazarian, S. G.; Salter, P. A.; Welton, T. Molecular States of Water in Room Temperature Ionic Liquids. *Phys. Chem. Chem. Phys.* **2001**, *3*, 5192−5200.
(19) Terranova, Z. L.; Corcelli, S. A. Molecular Dynamics Investigation of the Vibrational Spectroscopy of Isolated Water in an Ionic Liquid. *J. Phys. Chem. B* **2014**, *118*, 8264−8272.
(20) Kramer, P. L.; Giammanco, C. H.; Fayer, M. D. Dynamics of Water, Methanol, and Ethanol in a Room Temperature Ionic Liquid. *J. Chem. Phys.* **2015**, *142*, 212408.
(21) Falk, M. An Infrared Study of Water in Perfluorosulfonate (Nafion) Membranes. *Can. J. Chem.* **1980**, *58*, 1495−1501.
(22) Moilanen, D. E.; Piletic, I. R.; Fayer, M. D. Water Dynamics in Nafion Fuel Cell Membranes: The Effects of Confinement and Structural Changes on the Hydrogen Bonding Network. *J. Phys. Chem. C* **2007**, *111*, 8884−8891.
(23) Shimizu, A.; Taniguchi, Y. NMR Studies of Reorientational Motion of Hydrated D_2O Molecules of Halide Ions (F^-, Cl^-, Br^-, and I^-) in Dilute Aqueous Solutions. *Bull. Chem. Soc. Jpn.* **1991**, *64*, 1613−1617.
(24) Fayer, M. D.; Moilanen, D. E.; Wong, D.; Rosenfeld, D. E.; Fenn, E. E.; Park, S. Water Dynamics in Salt Solutions Studied with Ultrafast Two-Dimensional Infrared (2D IR) Vibrational Echo Spectroscopy. *Acc. Chem. Res.* **2009**, *42*, 1210−1219.
(25) Kropman, M. F.; Bakker, H. J. Effect of Ions on the Vibrational Relaxation of Liquid Water. *J. Am. Chem. Soc.* **2004**, *126*, 9135−9141.
(26) Smith, J. D.; Saykally, R. J.; Geissler, P. L. The Effect of Dissolved Halide Anions on Hydrogen Bonding in Liquid Water. *J. Am. Chem. Soc.* **2007**, *129*, 13847−13856.
(27) Moilanen, D. E.; Wong, D.; Rosenfeld, D. E.; Fenn, E. E.; Fayer, M. D. Ion-Water Hydrogen-Bond Switching Observed with 2D IR Vibrational Echo Chemical Exchange Spectroscopy. *Proc. Natl. Acad. Sci. U. S. A.* **2009**, *106*, 375−380.
(28) Raugei, S.; Klein, M. L. An *Ab Initio* Study of Water Molecules in the Bromide Ion Solvation Shell. *J. Chem. Phys.* **2002**, *116*, 196−202.
(29) Chowdhuri, S.; Chandra, A. Dynamics of Halide Ion-Water Hydrogen Bonds in Aqueous Solutions: Dependence on Ion Size and Temperature. *J. Phys. Chem. B* **2006**, *110*, 9674−9680.
(30) Chandra, A. Dynamical Behavior of Anion-Water and Water-Water Hydrogen Bonds in Aqueous Electrolyte Solutions: A Molecular Dynamics Study. *J. Phys. Chem. B* **2003**, *107*, 3899−3906.
(31) Mason, P. E.; Neilson, G. W.; Dempsey, C. E.; Barnes, A. C.; Cruickshank, J. M. The Hydration Structure of Guanidinium and Thiocyanate Ions: Implications for Protein Stability in Aqueous Solution. *Proc. Natl. Acad. Sci. U. S. A.* **2003**, *100*, 4557−4561.
(32) Mancinelli, R.; Botti, A.; Bruni, F.; Ricci, M. A.; Soper, A. K. Hydration of Sodium, Potassium, and Chloride Ions in Solution and the Concept of Structure Maker/Breaker. *J. Phys. Chem. B* **2007**, *111*, 13570−13577.
(33) Kameda, Y.; Takahashi, R.; Usuki, T.; Uemura, O. Hydration Structure of SCN^- in Concentrated Aqueous Sodium Thiocyanate Solutions. *Bull. Chem. Soc. Jpn.* **1994**, *67*, 956−963.
(34) Cappa, C. D.; Smith, J. D.; Wilson, K. R.; Messer, B. M.; Gilles, M. K.; Cohen, R. C.; Saykally, R. J. Effects of Alkali Metal Halide Salts on the Hydrogen Bond Network of Liquid Water. *J. Phys. Chem. B* **2005**, *109*, 7046−7052.
(35) Naslund, L. A.; Edwards, D. C.; Wernet, P.; Bergmann, U.; Ogasawara, H.; Pettersson, L. G. M.; Myneni, S.; Nilsson, A. X-Ray Absorption Spectroscopy Study of the Hydrogen Bond Network in the Bulk Water of Aqueous Solutions. *J. Phys. Chem. A* **2005**, *109*, 5995−6002.
(36) Park, K. H.; Choi, S. R.; Choi, J. H.; Park, S.; Cho, M. Real-Time Probing of Ion Pairing Dynamics with 2DIR Spectroscopy. *ChemPhysChem* **2010**, *11*, 3632−3637.
(37) Bian, H.; Wen, X.; Li, J.; Zheng, J. Mode-Specific Intermolecular Vibrational Energy Transfer. II. Deuterated Water and Potassium Selenocyanate Mixture. *J. Chem. Phys.* **2010**, *133*, 034505-1−034505-15.
(38) Schmidt, J. R.; Corcelli, S. A.; Skinner, J. L. Pronounced Non-Condon Effects in the Ultrafast Infrared Spectroscopy of Water. *J. Chem. Phys.* **2005**, *123*, 044513.
(39) Loparo, J. J.; Roberts, S. T.; Nicodemus, R. A.; Tokmakoff, A. Variation of the Transition Dipole Moment across the OH Stretching Band of Water. *Chem. Phys.* **2007**, *341*, 218−229.
(40) Karthick Kumar, S. K.; Tamimi, A.; Fayer, M. D. Comparisons of 2D IR Measured Spectral Diffusion in Rotating Frames Using Pulse Shaping and in the Stationary Frame Using the Standard Method. *J. Chem. Phys.* **2012**, *137*, 184201.
(41) Kwak, K.; Park, S.; Finkelstein, I. J.; Fayer, M. D. Frequency-Frequency Correlation Functions and Apodization in Two-Dimensional Infrared Vibrational Echo Spectroscopy: A New Approach. *J. Chem. Phys.* **2007**, *127*, 124503.
(42) Kwak, K.; Rosenfeld, D. E.; Fayer, M. D. Taking Apart the Two-Dimensional Infrared Vibrational Echo Spectra: More Information and Elimination of Distortions. *J. Chem. Phys.* **2008**, *128*, 204505.
(43) Hauser, H.; Haering, G.; Pande, A.; Luisi, P. L. Interaction of Water with Sodium Bis(2-Ethyl-1-Hexyl) Sulfosuccinate in Reversed Micelles. *J. Phys. Chem.* **1989**, *93*, 7869−7876.

DOI: 10.1021/acs.jpcb.5b08168
J. Phys. Chem. B 2015, 119, 13407−13415

(44) Faeder, J.; Ladanyi, B. M. Molecular Dynamics Simulations of the Interior of Aqueous Reverse Micelles. *J. Phys. Chem. B* **2000**, *104*, 1033−1046.
(45) Lawrence, C. P.; Skinner, J. L. Vibrational Spectroscopy of HOD in Liquid D_2O. III. Spectral Diffusion, and Hydrogen-Bonding and Rotational Dynamics. *J. Chem. Phys.* **2003**, *118*, 264−272.
(46) Lindquist, B. A.; Corcelli, S. A. Nitrile Groups as Vibrational Probes: Calculations of the C N Infrared Absorption Line Shape of Acetonitrile in Water and Tetrahydrofuran. *J. Phys. Chem. B* **2008**, *112*, 6301−6303.
(47) Corcelli, S. A.; Lawrence, C. P.; Asbury, J. B.; Steinel, T.; Fayer, M. D.; Skinner, J. L. Spectral Diffusion in a Fluctuating Charge Model of Water. *J. Chem. Phys.* **2004**, *121*, 8897−8900.
(48) Pimentel, G. C.; McClellan, A. L. Hydrogen Bonding. *Annu. Rev. Phys. Chem.* **1971**, *22*, 347−385.
(49) Kropman, M. F.; Bakker, H. J. Dynamics of Water Molecules in Aqueous Solvation Shells. *Science* **2001**, *291*, 2118−2120.

DOI: 10.1021/acs.jpcb.5b08168
J. Phys. Chem. B 2015, 119, 13407−13415